Coopersmith Kaitlin (Orcid ID: 0000-0001-6589-8825)

Rapid paper spray mass spectrometry characterization of uranium and exemplar molecular species.

Kaitlin Coopersmith (Kaitlin.Lawrence@srnl.doe.gov)[1], Robert B. Cody (cody@jeol.com)[2], Joseph M. Mannion (Joseph.Mannion@srnl.doe.gov)[1], Joshua T. Hewitt (Joshua.Hewitt2@dodiis.mil)[1], Samuel B. Koby (sbk23@pitt.edu)[1], Matthew S. Wellons (Matthew.Wellons@srnl.doe.gov)[1*]

1. Savannah River National Laboratory, P.O. Box A, Aiken, South Carolina 29808, USA
2. JEOL USA, Inc., Peabody, MA 01960, USA

*Corresponding Author: Email: Matthew.Wellons@srnl.doe.gov; Tel: +1 (803) 725-0412

Keywords: Mass spectrometry, paper spray ionization, uranium detection, whole molecule detection, isotopic analysis

Abstract

RATIONALE: The ability to detect and quantify the presence of specific inorganic elements and complexes is essential for environmental monitoring and nuclear safeguards applications. In this work, paper spray ionization mass spectrometry (PSI-MS) was used for the rapid chemical and isotopic characterization of trace inorganic species collected on cotton swipe substrates. The direct analysis of cotton swipes using this ambient ionization technique led to fast sample analysis that retained original chemical information of the source material with minimal sample preparation.
METHODS: Mass spectra were collected on an atmospheric pressure ionization, high-resolution mass spectrometer for solutions containing uranyl acetate, uranyl chloride, uranyl nitrate, and uranyl tri-*n*-butylphosphate (uranyl-TBP) complexes. Gadolinium nitrate was used as an internal standard for the quantitative analysis of uranium. To demonstrate the ability to characterize inorganic contaminants in the presence of uranium, a multi-element inorganic standard containing U, Bi, Pb, Cd, Fe, and Zn was deposited onto cotton substrates and directly analyzed without purification.
RESULTS: All elements doped on the cotton substrate were detected with strong signal-to-noise (S/N) ratios (S/N~1000 for UO_2^+ on multi-element doped swipes) and high integrated intensities (>10^5 counts) from collection periods of approximately 1 min. Limits of detection were determined to be approximately 94 ng for UO_2^+ and uranyl acetate through the measurement of ppb level solutions.
CONCLUSIONS: The rapid analysis of uranium and other inorganic-containing samples while still retaining original chemical information (e.g. uranyl complexation) was demonstrated. Qualitative detection and speciation were achieved in less than 1 min of analysis. For uranium isotopic quantitation, longer accumulations (>15 min) can be sustained to improve the accuracy of minor ^{235}U isotopic abundance measurements to approximately 1% error.

This article has been accepted for publication and undergone full peer review but has not been through the copyediting, typesetting, pagination and proofreading process which may lead to differences between this version and the Version of Record. Please cite this article as doi: 10.1002/rcm.8517

INTRODUCTION

The characterization of actinides within environmentally collected samples is paramount for efforts in environmental monitoring,[1-2] nuclear forensics,[3-5] and nuclear safeguards.[6-9] Specifically, isotopic and molecular information of actinides can be used to monitor treaty verification or determine the intended use of the material.[10] The presence of undeclared activities is a worldwide concern; in 2017, there were 139 confirmed incidents related to the unauthorized transport of radioactive sources or radioactively contaminated materials reported by the Incident and Trafficking Database (ITDB).[11] Thus, to ensure the peaceful use of nuclear materials, the ability to accurately detect low levels of actinides and the presence of artificial isotopes while retaining original molecular information is vital.

The chemical speciation of actinides or concurrent organic species can provide clues about the geological origin of the material,[9] the intent or history of the material, and offer an additional axis for forensic fingerprinting.[8,12] For example, the presence of uranyl tri-*n*-butyl phosphate (uranyl-TBP) complexes may indicate concurrent reprocessing efforts,[13] or the state of hydrolysis could be used to determine the age or history of the material.[14] Ideal detection capabilities for the determination of nuclear materials include the retention of molecular information, minimal sample preparation, and small sample requirements to minimize waste and reduce the radioactivity of highly hazardous material.

Various analytical techniques that are typically used for uranium detection include radiometric techniques (e.g. α- and γ- spectroscopy)[15], microscopy-based techniques (e.g. energy dispersive x-ray microanalysis)[16], and mass spectrometry (e.g. multi-collector inductively coupled plasma mass spectrometry (ICP-MS) and ion mobility spectrometry).[8-10, 17-20] A shortcoming of current analytical paradigms is the lack of chemical information provided by these analyses. For example, techniques that require harsh sample preparations and instrumental conditions, such as with ionization with a plasma torch, actinide speciation is lost. Most MS techniques, such as ICP-MS or thermal ionization MS, have stronger ionization sources that lose chemical speciation information. In other techniques, such as SEM-EDS or γ-spectroscopy, the isotopic or chemical information is inherently non-discernable by the nature of the technique.[21] In addition, most mass spectrometry techniques on substrates require the digestion of the entire sample and substrate, which increases the complexity of the analysis.[10]

Mass spectrometry has long been recognized as one of the most sensitive methods for the characterization of long-lived actinides, but these techniques have been used primarily for the quantitation of isotopic ratios[20,22] or the characterization of inorganic contaminates[3, 12] rather than the identification and quantification of specific inorganic complexes. Paper spray ionization MS (PSI-MS), and the closely related swab touch spray ionization MS,[23] have recently gained attention as versatile, ambient ionization techniques requiring minimal sample preparation and sample consumption for the direct analysis of blood,[24-26] urine,[27-28] and environmentally collected chemical warfare agent simulants.[29] In PSI-MS, the sample is transferred onto a substrate, which is then wetted with solvent while exposed to a high electrical potential to induce electrospray ionization directly from the substrate. The substrate is used to load the sample, extract the analyte, and generate the spray ionization.[30] The solvent and substrate can be optimized to enhance the sensitivity and specificity of the detection of analytes. PSI-MS has several advantages over other comparable analytical techniques (e.g. LC/ESI-MS) including reduced sample preparation, rapid processing, and reduced carryover. In addition, chemical speciation is retained because ionization is “soft” and the sample is only solvated immediately prior to analysis, which minimizes the potential for in-solution chemical transformations. Ion mobility spectrometry (IMS) also uses a soft ionization source and can detect gas-phase ions based on their mobility in a gas; however, the detection limits are typically lower than those for PSI-MS, and the drift time needs to be calibrated or the drift tube coupled to a mass spectrometer.[19] In addition, IMS has not been used to identify whole molecule inorganic complexes with organic ligands, a method which is used to establish the intended use of the material for treaty verification.[19] Compared with nanoelectrospray ionization, the internal energies of the ions generated through paper spray ionization are slightly lower, leading to better retention of molecular species.[30]

These advantages of PSI-MS would strengthen inorganic measurement capabilities in several regards; first, the elimination of sample preparation would greatly expedite sample turnaround, allowing for timelier sample analysis. Second, PSI-MS could be integrated into an environmental sampling paradigm while preserving the chemical information captured on swipes, including the identity and presence of organics;[31-32] molecular information on the nuclear materials provide additional clues regarding the operation of a facility or the intended use of material. Third, the reduced cost and time associated with analyses would allow for a greater number of measurements to be conducted, improving the likelihood of the detection of nuclear activities. In this communication, PSI-MS is demonstrated as a versatile tool for the rapid and simultaneous analysis of organic, inorganic, and coordination complex species in support of nuclear safeguards efforts.

EXPERIMENTAL

Reagents. All chemicals were used as received. Single element 1000 ppm high purity standards of Bi, Cd, Pb, Fe, Zn, Gd and U in nitric acid were purchased from High-Purity Standards, Inc. in North Charleston SC, USA. Polypropylene glycol monoamine with a molecular weight of 600 g/mol (Jeffamine M-600) was purchased from Huntsman in The Woodlands, TX, USA. Uranyl acetate, nitric acid, and tri-*n*-butylphosphate (TBP) were purchased from Sigma-Aldrich (St. Louis MO, USA). The substrates that were used for these tests include the Texwipe 304 (cotton swipes and wedges) and grade 2 Whatman cellulosic filter paper (paper wedges) purchased from Fisher Scientific (Waltham, MA, USA).

Multi-element doped cotton swipe preparation. High purity single element 1000 ppm standards of Bi, Cd, Pb, Fe, and Zn in 0.5 M nitric acid were sequentially deposited (250 µL) on cotton swipes. A 1000 ppm depleted uranium standard in 8 M nitric acid was then deposited (250 µL). Each deposition was fully dried before the deposition of the subsequent solution. Swipes were prepared in a Class I clean room and depositions were limited to a region ~4 cm in diameter on the swipe. Prepared swipes were then individually packaged in sealed polyethylene bags and shipped to JEOL labs (Peabody, MA, USA) for analysis.

Instrument Methodology and Operation. All samples were analyzed with a JEOL AccuTOF™ DART® 4G mass spectrometer at JEOL labs in Boston, MA, USA. The JEOL paper spray ion source, which consists of a copper clamp, safety interlock and manual positioning system, was used for these analyses. The radiofrequency quadrupole ion guide was set to an amplitude of 1000 V for high-mass mode to exclude ions with $m/z < 100$, and an amplitude of 100 V was used for low-mass mode to detect low-mass ions with $m/z > 12$. Cone ("orifice 1") voltages between 20 and 80 V were tested; higher cone voltages were used to induce ion fragmentation. The paper spray source was held at +3.0 kV for positive-ion mode and -3.0 kV for negative-ion mode. Paper and cotton wedges were cut from the swipes to ~2 cm in length with care given to produce a fine point. Paper and cotton wedges were positioned ~1.5 cm from the skimmer cone entrance and aligned manually during the first ~30 s of the run. The total ion current chronogram was used during the alignment process to maximize the ion current into the mass spectrometer. A methanol/water mixture (80/20) was used as a makeup solvent and was applied dropwise at the back of the paper wedges using a syringe pump to prevent the paper from drying and extend the duration of ion signals. The solvent flow rate was estimated to be 8 µL/min and was started at the beginning of each run. Version 4 of msAxel software (JEOL USA Inc) was used for data acquisition and mass calibration, and to export spectrum data from regions of interest in the extracted ion current chromatogram (EICC). JeffamineM-600 was analyzed at the end of each run as an external mass reference standard for exact mass measurements. Mass Mountaineer software (Fineview, NY, USA*)* was used for peak identification. Peak deconvolution was carried out in OriginPro2016 (OriginLab Corporation, Northampton, MA, USA) using the second derivative to obtain peak locations and intensities.

Sample Analyses. In cases where swipe samples were directly analyzed, wedges of the swipe material were cut, mounted in the source, and solvated with an 80/20 methanol/water mixture using a syringe pump. For the analysis of uranium-containing whole molecule complexes, 7 µL of the U-containing solution were deposited near the center of paper wedges, mounted in the source and immediately solvated by the syringe pump. Measurements of uranyl acetate and uranyl chloride were performed with the respective solutions without modification from the manufacturer. In the case of uranyl-TBP complex characterization, uranyl nitrate was prepared from uranyl acetate through the addition of nitric acid. Uranyl nitrate (200 µL at 0.2 µM) was mixed with TBP (200 µL at 0.5 µM). After ~5 min at room temperature, the mixture was deposited onto the filter paper wedges and analyzed.

Introduction of Gadolinium as an Internal Standard for Quantitation. Gadolinium nitrate ($Gd(NO_3)_3$) was added to solutions of uranyl chloride as an internal standard. Solutions were prepared such that a constant gadolinium concentration of 50 ppm was maintained for all uranyl concentrations, which ranged from 0.5 ppm to 250 ppm. The solutions were added to filter paper wedges (7 µL) and solvated with 8 µL/min 80/20 methanol/water. The quotient of the $[^{238}U^{16}O_2]^+$ and $[^{160}Gd^{16}O]^+$ intensity, at *m/z* 270.0406 and 175.9220, respectively, was plotted versus the concentration of loaded uranyl to form a calibration curve, which was used to calculated the detection limit (DL) in ppm using equation 1:

$$DL = \frac{3 * \sqrt{\frac{\Sigma(y_i - y_{calc})^2}{N-2}}}{b} \tag{1}$$

where y_i is the intensity value at the different concentrations, y_{calc} is the predicted intensity value based on the best fit line of the calibration curve, N is the number of runs, and b is the slope of the calibration curve.

RESULTS/DISCUSSION

Cotton and paper swipes were doped with multielement standards and uranium compounds, respectively, and analyzed using PSI-MS. The identification of whole molecule uranium compounds was observed, and the quantification of uranium was possible through the addition of a gadolinium internal standard. As demonstrated previously with ESI-MS, solvent selection for the analysis of actinide compounds can influence the type of ions formed due to solubility, chemical interactions between the solvent and formed ions, and the formation of adduct ions with solvent molecules.[33-34] Water was found to be a poor solvent for uranyl and uranyl-bearing complexes; therefore, the use of a methanol and water mixture improved sensitivity for uranyl several orders of magnitude compared with water alone.

Analysis of Uranium and Multi-Element Specimens.

Direct analysis of cotton swipes doped with a multi-element mix showed that all elements in the matrix (U, Bi, Pb, Cd, Fe, and Zn) could be detected in positive-ion mode (Figure 1). The only sample preparation required for this technique involves cutting a wedge of the swipe material and solvent addition via syringe pump. Although only 250 µg of each element were deposited on the cotton substrate, all species demonstrated strong signal to noise with high integrated intensities ($>10^5$ counts) from collection periods of approximately 1 min. Direct analysis of multi-element swipes was repeated 7 times and uranyl was detected in all cases. The transition elements were detected as single element cations while uranium was always present as a uranyl ($[UO_2]^+$) cation. The measured isotope abundances were in good agreement with natural abundances for most of the major isotopes, indicating a low organic background from the cotton swipes at the desired *m/z* values (Tables S1 and S2, supporting information). Negative-ion mode was not useful for the detection of transition elements due to the high abundance of negative adducts; however, the 1:2 and 1:3 uranyl-nitrate complexes were detected (Figure 2). Uranyl-nitrate complexes were not detected in positive-ion mode despite modulation of cone voltages, suggesting that this behavior is due to ionization mechanisms rather than fragmentation.

Positive-ion mass spectra were collected in both high- and low-mass instrument collection schemes. Low-mass operation mode was used to detect a wide range of elements with *m/z* > 12. Low-mass operation mode demonstrated the detection of the U, Bi, Pb, Cd, Fe, and Zn elements doped on the cotton substrate. Ca from the cotton substrate, and O from atmosphere were also detected (Figure 1A). High-mass mode omits the *m/z* < 100 spectral range through alteration of the radiofrequency quadrupole ion guide amplitude, increasing the sensitivity for species with *m/z* > 100 through exclusion of lower mass ions.[35] Only Cd, Pb, Bi, and U were detected in high-mass mode, corresponding to omission of elements with *m/z* < 100 (Figure 1B). High-mass mode operation resulted in approximately one order of magnitude increase in the Pb, Bi, and uranyl cation count intensity. The errors in the measured isotopic abundances compared with the natural abundances were dependent on the measurement conditions and signal strength, as expected. For example, a lower error in the measured isotopic abundances for the more naturally occurring isotopes is observed due to the higher counts for the more abundant isotopes. In addition, the higher mass elements had a lower error in the high-mass mode; the measured isotopic abundances for the uranyl ion were closer to the natural abundance in the high-mass mode, where the instrument sensitivity is better for *m/z* > 100 (Table S2, supporting information).

Uranyl quantitation using gadolinium nitrate as an internal standard was carried out in high-mass mode to improve instrument sensitivity for U and Gd. A series of positive-ion mass spectra was collected from cellulosic filter paper that contained 50 ppm gadolinium nitrate co-deposited with various concentrations of uranyl. Gd was exclusively detected as the $[GdO]^+$ cation. The ratio of the measured $[^{238}U^{16}O_2]^+$ to $[^{160}Gd^{16}O]^+$ intensity was plotted against the deposited uranyl concentration to construct a calibration curve (Figure 3B). A linear relationship ($R^2=0.9944$) between the measured intensity and the deposited uranyl concentration was observed, and a detection limit of 18.8 ppm (94 ng) of $^{238}U^{16}O_2$ was calculated. This demonstrates that PSI-MS is a promising technique for the detection of nanogram levels of uranyl with minimal sample preparation. At equivalent concentrations, the intensity of $[^{160}Gd^{16}O]^+$ is approximately 20% that of $[^{238}U^{16}O_2]^+$ (Table S3, supporting information), indicating similar ionization efficiencies between the oxides of Gd and U based on the natural isotope abundance of ^{160}Gd (21.5%).

Current limitations on the detection capabilities for the quantitation of the less abundant uranyl isotopes using PSI-MS include the presence of an interfering peak at *m/z* 267.002, which neighbors $[^{235}U^{16}O_2]^+$ with *m/z* 267.0338 (Figures S1 and S2, supporting information). Peak deconvolution shows that the quotient of the sample peak and the interfering peak becomes more biased towards the interfering peak below 50 ppm (Figure S1B), indicating that the peak is an interference from a background species and not a uranium species. Comparing the different isotopes of Gd in the spectrum also indicates that this peak is not an interference of the internal standard. As the concentration increased, the relative intensity of the peak decreased; however, at the lowest concentrations, peak deconvolution was carried out to obtain the intensities for the calibration curve. The identity of the interfering species will be resolved in future work but is possibly an interference in the substrate. Tables S4 and S5 (supporting information) summarize the results from the extracted intensity values.

The use of PSI-MS for uranium isotope ratio measurements was assessed from a series of positive-ion mass spectra collected from cellulosic filter paper with 50 ppm uranyl deposited as described in the experimental section. Natural uranium was used in all isotope ratio trials. The measured $[^{235}U^{16}O_2]^+/[^{238}U^{16}O_2]^+$ ratio was compared with the natural ^{235}U abundance of 0.720% and a percentage error was calculated (Figure 4). The percentage error in the measured isotope ratio was found to correlate to the number of collected uranium ion counts for a given trial, with higher counts correlating to lower error until the signal was above $\sim 4\text{x}10^6$ accumulated $[UO_2]^+$ ion counts, where the sample intensity exceeded the range of the detector. Trials with higher accumulated uranyl counts correspond to longer accumulation periods. Accumulation periods between 1 and 15 minutes were investigated. Based on the measured relationship between accumulated $[UO_2]^+$ counts and isotope ratio error, less than 1% error can be expected for trials with ion counts of the order of $\sim 10^6$ for a given uranium-bearing species. The effect of substrate material on the percentage error was not quantitatively analyzed in this work; however, the cotton swipes were found to produce more stable ion counts than cellulosic filter paper. We believe this behavior is due to better solvent retention in the cotton swipes than on the filter paper. It is expected that the choice of substrate will have a small effect on the error, either by affecting signal stability or through matrix effects.

Analysis of Uranium-containing Whole Molecule complexes

Mass spectra were collected for solutions containing uranyl acetate, uranyl chloride, uranyl nitrate, and uranyl-TBP complex deposited on cellulosic filter paper as described in the experimental section. High-mass mode was used for all uranyl coordination complex analyses to improve the sensitivity for uranyl-bearing complexes. Negative-ion and positive-ion instrument collection modes were both tested for each target species. Preliminary results for the measurements of 0.1 ppm of uranyl acetate, chloride, and nitrate demonstrated detection of nitrate and acetate into the ppb range and nanogram uranium mass quantities (Figures 2 and 5). All attempts to detect the whole uranyl chloride ion complex only yielded uranyl ions despite attempts to modulate cone voltages to prevent fragmentation. Both uranyl acetate and nitrate were detected as whole molecular clusters in negative-ion mode, but not in positive mode.

Uranyl-TBP complexes were prepared by mixing the TBP ligand with uranyl nitrate and then directly depositing small volumes onto the paper substrate. The 1:2 and 1:3 uranyl-TBP complexes were detected in positive-ion mode alongside TBP-Na adducts and the uranyl cation (Figure 6 and Table 2). No uranyl-TBP complexes were observed in negative-ion mode; however, the 1:2 and 1:3 uranyl-nitrate complexes were observed. These findings are similar to those reported by PNNL for ESI-MS characterization of aqueous uranyl-TBP mixtures, although several differences were observed.[36] At low cone voltages (20 V) only the 1:3 uranyl-TBP complex was observed in the ESI mass spectrum and no un-bound uranyl was detected. Unbound TBP and TBP dimers were detected in the positive ESI mass spectrum which were not present in the PSI mass spectrum at an equivalent cone voltage. The presence of free uranyl and the 1:2 uranyl-TBP complex in the positive PSI mass spectrum does not appear to be a product of fragmentation due to the absence of the 1:1 uranyl-TBP species and may be the result of short equilibration times or interaction with the substrate.

CONCLUSION/SUMMARY

PSI-MS is demonstrated to be a promising technique for applications in nuclear safeguards and environmental monitoring for both qualitative and quantitative uranium analysis. In addition, PSI-MS has been demonstrated to detect other inorganic species on a cotton substrate. Circumvention of harsh sample preparations and minimization of solvent exposure afford PSI-MS a unique advantage over other MS techniques in the characterization of whole uranium molecules. Future studies will focus on the feasibility of direct analysis of environmentally collected samples and the applicability of PSI-MS to other coordination complexes of interest. Development of substrates with improved solvent retention may improve the stability of ion currents and prolong accumulation periods, which would benefit isotopic analyses. The effects of solvent selection and differences between ESI-MS and PSI-MS spectra warrant further investigation. For example, solvent selection has been shown to affect ESI-MS based on solubility and interactions with the analyte.[33-34]

ACKNOWLEDGEMENTS

This manuscript has been authored by Savannah River Nuclear Solutions, LLC under Contract No. DE-AC09-08SR22470 with the U.S. Department of Energy. The United States Government retains and the publisher, by accepting this article for publication, acknowledges that the United States Government retains a non-exclusive, paid-up, irrevocable, worldwide license to publish or reproduce the published form of this work, or allow others to do so, for United States Government purposes. Financial support for this work was provided by the SRNL Laboratory Directed Research & Development (LDRD) program through project number LDRD-2018-0004.

References:

1. Zheng J, Tagami K, Watanabe Y, et al. Isotopic evidence of plutonium release into the environment from the Fukushima DNPP accident. *Scientific Reports.* 2012;2(304):1-8.
2. Becker JS, Zoriy M, Halicz L, et al. Environmental monitoring of plutonium at ultratrace level in natural water (Sea of Galilee-Israel) by ICP-SFMS and MC-ICP-MS. *J Anal At Spectrom.* 2004;19(9):1257-1261.
3. Mayer K, Wallenius M, Ray I. Nuclear forensics-a methodology providing clues on the origin of illicitly trafficked nuclear materials. *Analyst.* 2005;130(4):433-441.
4. Kimura Y, Shinohara N, Funatake Y. Development of prototype nuclear forensics library for nuclear materials and radioisotopes in Japan Atomic Energy Agency. *Energy Procedia.* 2017;131:239-245.
5. Wallenius M, Mayer K. Age determination of plutonium material in nuclear forensics by thermal ionisation mass spectrometry. *Fresenius J Anal Chem.* 2000;366(3):234-238.
6. Boulyga S, Konegger-Kappel S, Richter S, Sangely L. Mass spectrometric analysis for nuclear safeguards. *J Anal At Spectrom.* 2015;30(7):1469-1489.
7. Donohue DL. Strengthening IAEA safeguards through environmental sampling and analysis. *J Alloys Compd.* 1998;271–273:11-18.
8. Suzuki D, Esaka F, Miyamoto Y, Magara M. Direct isotope ratio analysis of individual uranium–plutonium mixed particles with various U/Pu ratios by thermal ionization mass spectrometry. *Appl Radiat Isot.* 2015;96:52-56.
9. Spano TL, Simonetti A, Balboni E, Dorais C, Burns PC. Trace element and U isotope analysis of uraninite and ore concentrate: Applications for nuclear forensic investigations. *Appl Geochem.* 2017;84:277-285.
10. Boulyga SF, Koepf A, Konegger-Kappel S, Macsik Z, Stadelmann G. Uranium isotope analysis by MC-ICP-MS in sub-ng sized samples. *J Anal At Spectrom.* 2016;31(11):2272-2284.
11. *IAEA Annual Report 2017*. International Atomic Energy Agency: Vienna, Austria, 2017.
12. Švedkauskaite-LeGore J, Mayer K, Millet S, Nicholl A, Rasmussen G, Baltrunas D. Investigation of the isotopic composition of lead and of trace elements concentrations in natural uranium materials as a signature in nuclear forensics. *Radiochim Acta*, 2007;95(10):601-605.
13. Gillens AR, Powell BA. Rapid quantification of TBP and TBP degradation product ratios by FTIR-ATR. *J Radioanal Nucl Chem.* 2013;296(2):859-868.
14. Hu SW, Wang XY, Chu TW, Liu XQ. Theoretical Mechanism Study of UF6 Hydrolysis in the Gas Phase (II). *J Phys Chem A.* 2009;113(32):9243-9248.
15. Dewji SA, Lee DL, Hertel NE, Chapman JA, McElroy RD, Cleveland S. Validation of gamma-ray detection techniques for safeguards monitoring at natural uranium conversion facilities. *Nucl Instrum Methods Phys Res A.* 2016;823:135-148.
16. Hansson H, Pattersson HBL, Fortin C, Eriksson M. Uranium aerosols at a nuclear fuel fabrication plant: Characterization using scanning electron microscopy and energy dispersive X-ray spectroscopy. *Spectrochim Acta B.* 2017;131:130-137.
17. Forbes TP, Szakal C, Considerations for uranium isotope ratio analysis by atmospheric pressure ionization mass spectrometry. *Analyst.* 2019;144(1):317-323.
18. Fahey AJ, Groopman EE, Grabowski KS, Fazel KC. Measurement of uranium isotopes in particles of U3O8 by Secondary Ion Mass Spectrometry-Single Stage Accelerator Mass Spectrometry (SIMS-SSAMS). *Anal Chem.* 2016;88(14);7145-7153.
19. McLain DR, Steeb JL, Smith NA. Use of an ion mobility spectrometer for detecting uranium compounds. *Talanta.* 2018;184:227-234.

20. Taylor RN, Warneke T, Milton JA, Croudace IW, Warwick PE, Nesbitt RW. Plutonium isotope ratio analysis at femtogram to nanogram levels by multicollector ICP-MS. *J Anal At Spectrom.* 2001;16(3):279-284.

21. Liu W, Dai X, Bai Z, et al. Highly Sensitive and Selective Uranium Detection in Natural Water Systems Using a Luminescent Mesoporous Metal–Organic Framework Equipped with Abundant Lewis Basic Sites: A Combined Batch, X-ray Absorption Spectroscopy, and First Principles Simulation Investigation. *Environ Sci Technol.* 2017;51(7):3911-3921.

22. Aggarwal SK. Thermal ionisation mass spectrometry (TIMS) in nuclear science and technology - a review. *Anal Methods.* 2016;8(5):942-957.

23. Pirro V, Llor RS, Jarmusch AK, et al. Analysis of human gliomas by swab touch spray-mass spectrometry: applications to intraoperative assessment of surgical margins and presence of oncometabolites. *Analyst.* 2017;142(21):4058-4066.

24. Espy RD, Teunissen SF, Manicke NE, et al. Paper Spray and Extraction Spray Mass Spectrometry for the Direct and Simultaneous Quantification of Eight Drugs of Abuse in Whole Blood. *Anal Chem.* 2014;86(15):7712-7718.

25. Shi RZ, El Gierari ETM, Manicke NE, Faix JD. Rapid measurement of tacrolimus in whole blood by paper spray-tandem mass spectrometry (PS-MS/MS). *Clin Chim Acta.* 2015;441:99-104.

26. Jett R, Skaggs C, Manicke NE. Drug screening method development for paper spray coupled to a triple quadrupole mass spectrometer. *Anal Methods.* 2017;9(34):5037-5043.

27. Michely JA, Meyer MR, Maurer HH. Paper Spray Ionization Coupled to High Resolution Tandem Mass Spectrometry for Comprehensive Urine Drug Testing in Comparison to Liquid Chromatography-Coupled Techniques after Urine Precipitation or Dried Urine Spot Workup. *Anal Chem.* 2017;89(21):11779-11786.

28. Jeong ES, Kim KH, Cha E, Kwon OS, Cha S, Lee J. Direct and rapid quantitation of ephedrines in human urine by paper spray ionization/high resolution mass spectrometry. *J Chromatogr B.* 2016;1028:237-241.

29. Dhummakupt ES, Mach PM, Carmany D, et al. Direct Analysis of Aerosolized Chemical Warfare Simulants Captured on a Modified Glass-Based Substrate by “Paper-Spray” Ionization. *Anal Chem.* 2017;89(20):10866-10872.

30. Liu J, Manicke NE, Zhou X, Cooks RG, Ouyang Z. Paper Spray, In *New Developments in mass Spectrometry: Ambient Ionization Mass Spectrometry*, eds. Domin M, Cody R. The Royal Society of Chemistry: Cambridge UK; 2015:389-422.

31. Swindle DW Jr, Pearson RL, Wogman NA, Krey PW. Screening of potential sites for undeclared nuclear facilities in environmental monitoring for nuclear proliferation. *J Radioanal Nucl Chem.* 2001;248(3):599-604.

32. Wogman NA. Prospects for the introduction of wide area monitoring using environmental sampling for proliferation detection. *J Radioanal Nucl Chem.* 2013;296(2):1071-1077.

33. Somogy Á, Pasilis SP, Pemberton JE. Electrospray ionization of uranyl-citrate complexes: Adduct formation and ion-molecule reactions in 3D ion trap and ion cyclotron resonance trapping instruments. *Int J Mass Spectrom.* 2007;265(2-3):281-294.

34. Crawford CL, Fugate GA, Cable-Dunlap PR, Wall NA, Siems WF Jr, Hill HH. The novel analysis of uranyl compounds by electrospray-ion mobility-mass spectrometry. *Int J Mass Spectrom.* 2013;333:21-26.

35. Cody RB., Dane AJ. Paper spray ionization for ambient inorganic analysis. *Rapid Commun Mass Spectrom.* 2014;28(8):893-898.

36. McDonald LW, Campbell JA, Vercouter T, Clark SB. Characterization of Actinides Complexed to Nuclear Fuel Constituents Using ESI-MS. *Anal Chem.* 2016;88(5):2614-2621.

Table 1. Comparison of exact species masses with the measured masses observed using the negative-ion mode for the analysis of uranyl-acetate on filter paper.

Species	**Calculated *m/z***	**Measured *m/z***
$[(^{238}UO_2)(Ac)(O_2)]^-$	361.0438	361.0429
$[(^{238}UO_2)(Ac)_2]^-$	388.0672	388.0676
$[(^{238}UO_2)(Ac)_2(O_2)]^-$	420.0571	420.0656
$[(^{238}UO_2)(Ac)_3]^-$	447.0805	447.0724
$[(^{238}U_2O_4)(Ac)_3]^-$	749.1110	749.0982
$[(^{238}U_2O_4)(Ac)_4]^-$	776.1345	776.1198
$[(^{238}U_2O_6)(Ac)_4]^-$	808.1243	808.1094
$[(^{238}U_2O_4)(Ac)_5]^-$	835.1478	835.1313

Table 2. Comparison of exact species masses with the measured masses observed using the positive-ion high-mass mode for the analysis of aqueous uranyl-TBP mixtures.

Species	**Calculated *m/z***	**Measured *m/z***
$[^{238}U^{16}O_2]^+$	270.0406	270.0406
$[(TBP)Na]^+$	289.1544	289.1545
$[(TBP)_2Na_3{}^{16}OH]^+$	618.3033	618.3014
$[(^{238}U^{16}O_2)(TBP)_2N^{16}O_3]^+$	864.3586	864.3578
$[(TBP)_3Na_3{}^{16}OH]^+$	884.4682	884.4661
$[(^{238}UO_2)(TBP)_3N^{16}O_3]^+$	1130.5286	1130.5225

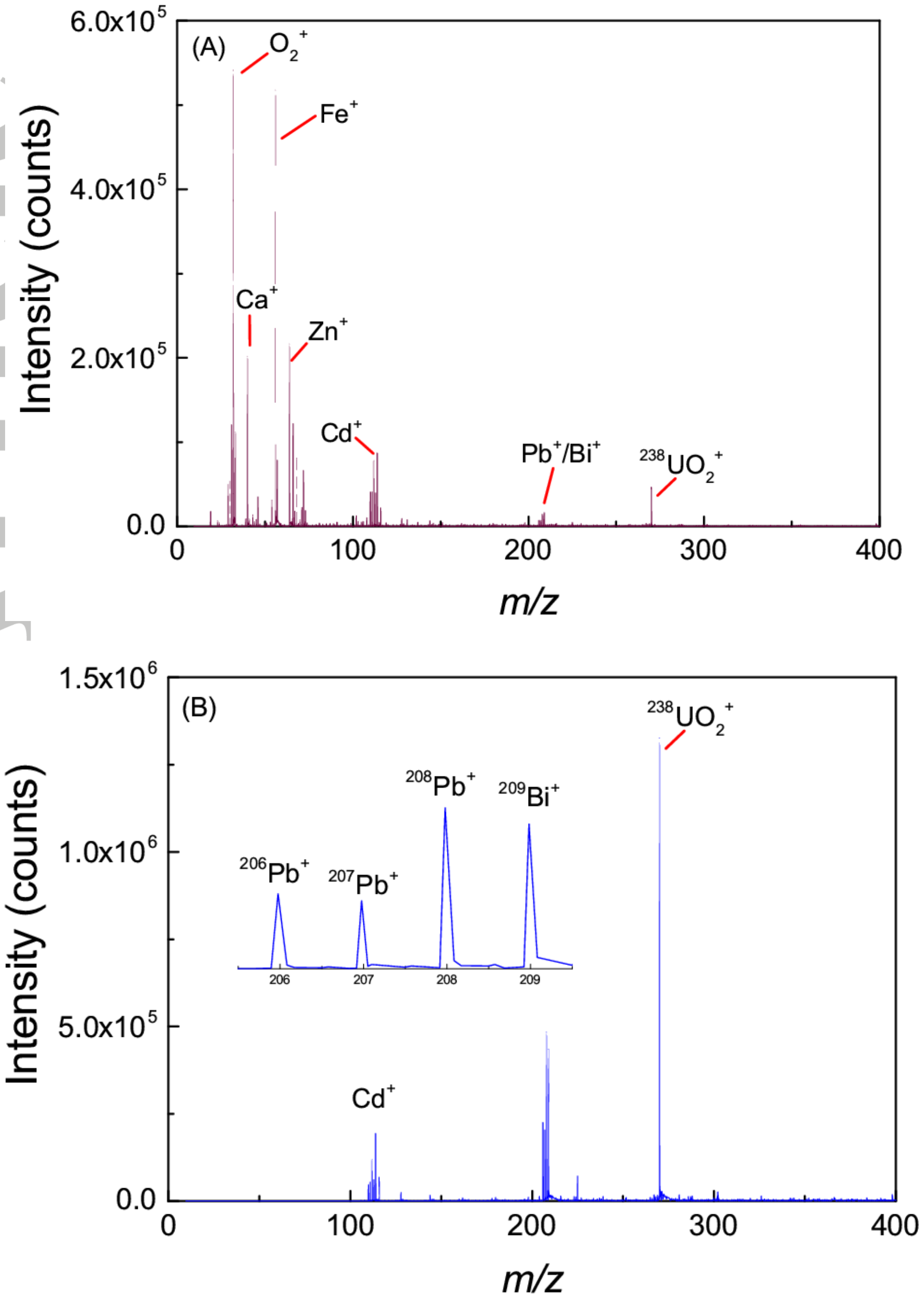

Figure 1. Positive-ion mass spectra of a directly analyzed multi-element doped cotton swipe in A) low-mass and B) high-mass modes. Complete identification of observed isotopes and the measured isotope abundances is provided in Tables S1 and S2 (supporting information).

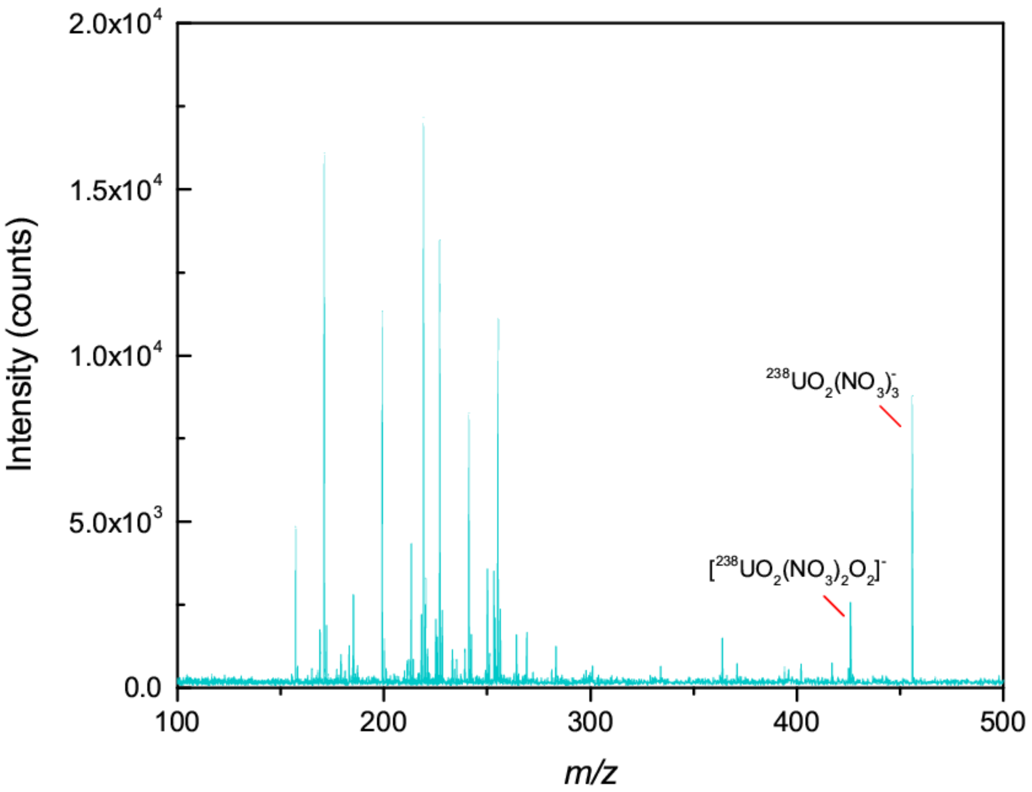

Figure 2. Negative-ion spectra of a directly analyzed multi-element doped cotton swipe in high-mass mode.

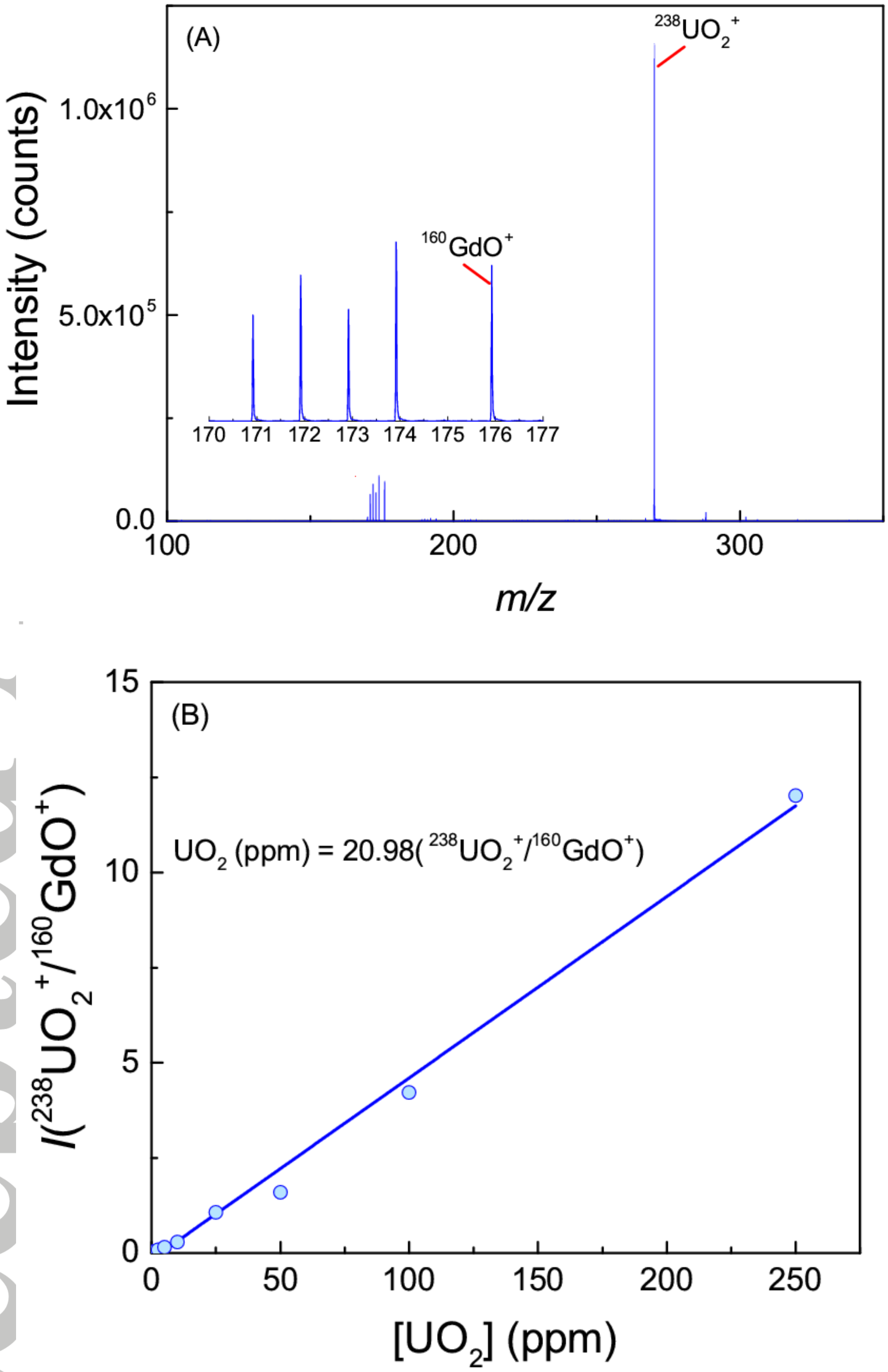

Figure 3. A) Positive-ion mass spectrum of solution containing 50 ppm UO_2Cl_2 and 50 ppm $Gd(NO_3)_3$ and B) linear calibration curve constructed from trials with 50 ppm Gd(NO3)3 as an internal standard and varying concentrations of UO_2Cl_2 (R^2=0.9944). Complete identification of observed isotopes and the measured isotope abundances is provided in Table S4 (supporting information).

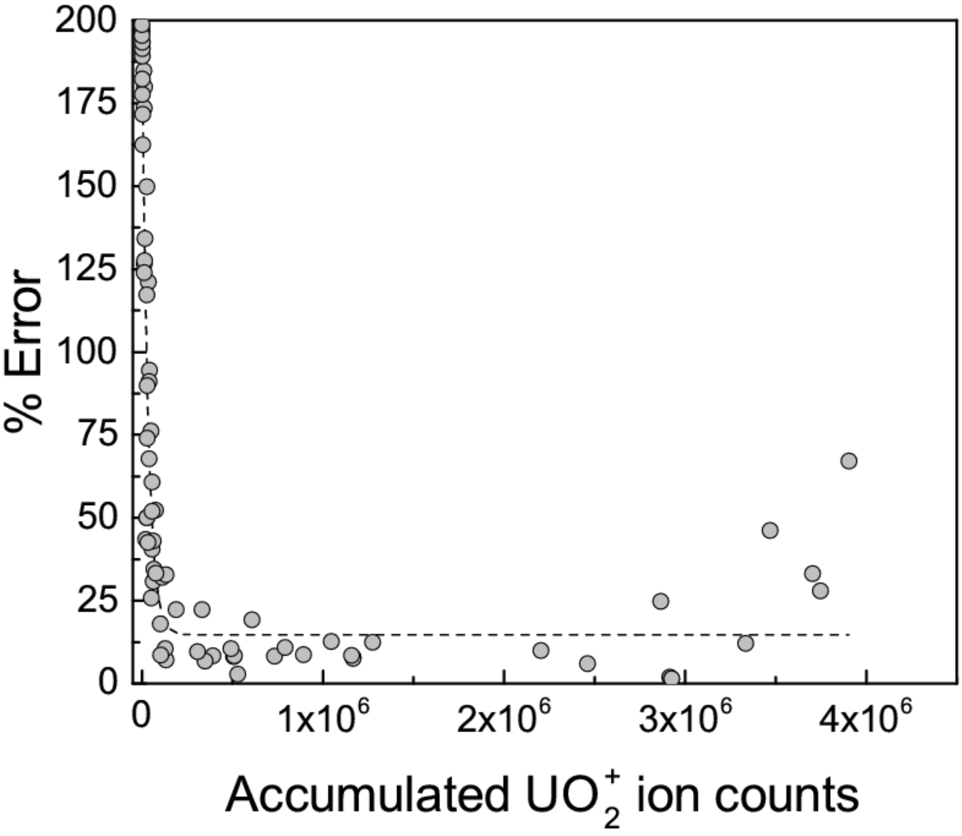

Figure 4. Relationship between the total accumulated intensity of $UO2^+$ (ion counts) and percentage error in the measured abundance of ^{235}U (natural ^{235}U abundance is 0.720%). Each data point represents one trial ranging in duration from 1 to 15 min. An increase in error at the higher counts is a result of the upper limit for the detector.

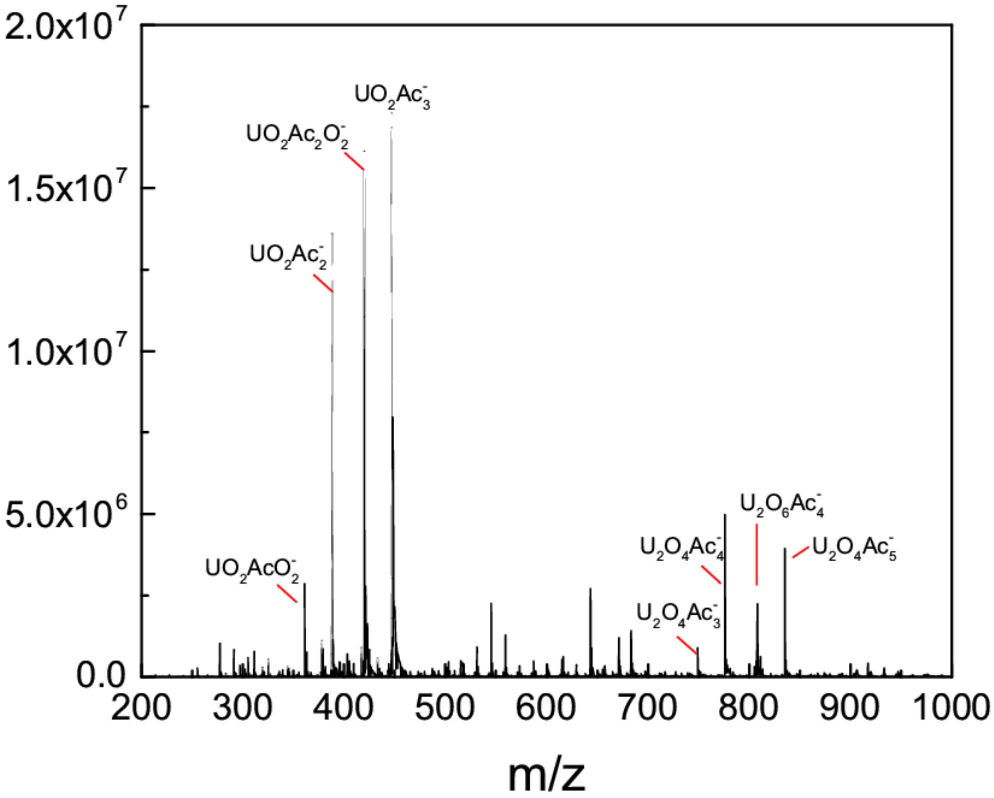

Figure 5. Negative-ion mass spectrum of uranyl acetate (UO$_2$Ac$_2$) deposited on filter paper. Complete identification of the observed species is provided in Table 1.

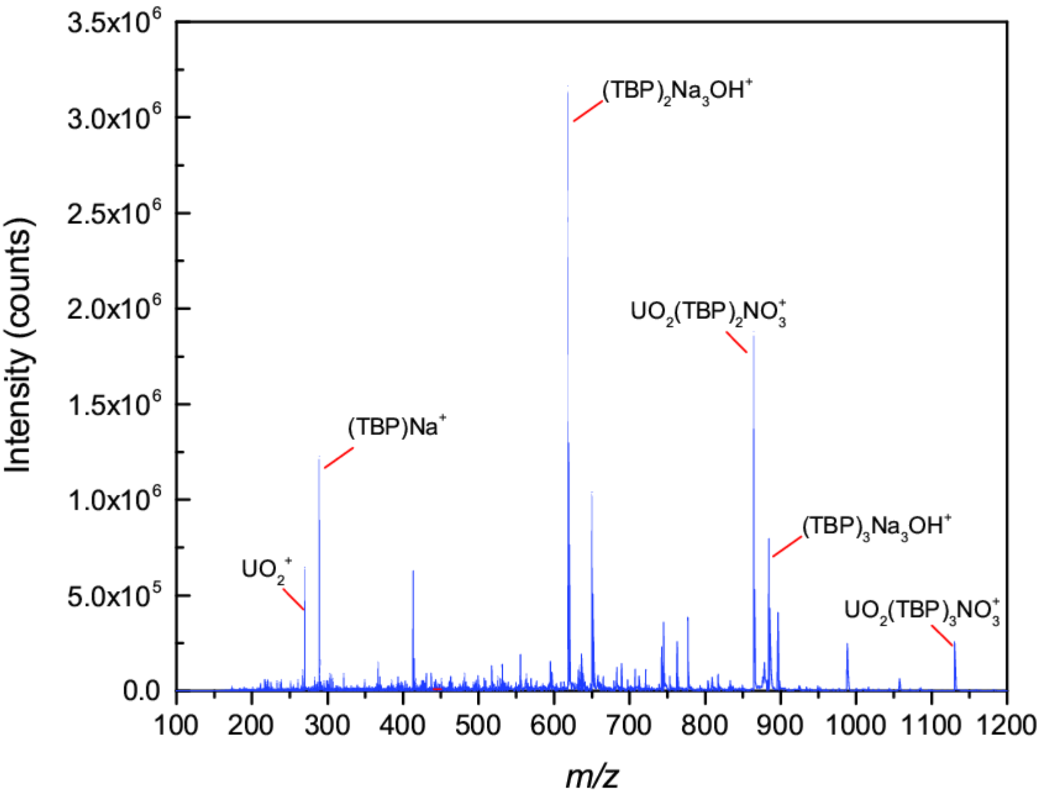

Figure 6. Positive-ion mass spectrum of 0.2 µM uranyl nitrate and 0.5 µM TBP deposited on (7 µL) on filter paper. Complete identification of the observed species is provided in Table 2.